Title

A rhodopsin in the brain functions in circadian photoentrainment in Drosophila

Journal

Nature, 545(7654)

ISSN

0028-0836

Authors

Ni, Jinfei D
Baik, Lisa S
Holmes, Todd C
et al.

Publication Date

2017-05-01

DOI

10.1038/nature22325

Peer reviewed

LETTER

doi:10.1038/nature22325

A rhodopsin in the brain functions in circadian photoentrainment in *Drosophila*

Jinfei D. Ni[1,2], Lisa S. Baik[3], Todd C. Holmes[3,4] & Craig Montell[1]

Animals partition their daily activity rhythms through their internal circadian clocks, which are synchronized by oscillating day–night cycles of light. The fruitfly *Drosophila melanogaster* senses day–night cycles in part through rhodopsin-dependent light reception in the compound eye and photoreceptor cells in the Hofbauer–Buchner eyelet[1]. A more noteworthy light entrainment pathway is mediated by central pacemaker neurons in the brain. The *Drosophila* circadian clock is extremely sensitive to light. However, the only known light sensor in pacemaker neurons, the flavoprotein cryptochrome (Cry)[2,3], responds only to high levels of light *in vitro*[4]. These observations indicate that there is an additional light-sensing pathway in fly pacemaker neurons[5]. Here we describe a previously uncharacterized rhodopsin, Rh7, which contributes to circadian light entrainment by circadian pacemaker neurons in the brain. The pacemaker neurons respond to violet light, and this response depends on Rh7. Loss of either *cry* or *rh7* caused minor defects in photoentrainment, whereas loss of both caused profound impairment. The circadian photoresponse to constant light was impaired in *rh7* mutant flies, especially under dim light. The demonstration that Rh7 functions in circadian pacemaker neurons represents, to our knowledge, the first role for an opsin in the central brain.

Cry is a light detector in central pacemaker neurons that contributes to phototrainment[3,6]. However, *cry* mutant flies still entrain to light–dark (L–D) cycles[3,6]. Therefore, we screened for an additional light sensor that functions in circadian photoentrainment using *Drosophila* activity monitors. We entrained flies under 12 h light–12 h dark (L–D) cycles for 4 days, and switched them to constant dark (D–D) conditions. Control flies (w^{1118}) displayed two daily activity peaks during dawn and dusk, termed the morning and evening peaks (Fig. 1a; note these are double plots). Activity increased before the light and dark transitions, indicating anticipation of changes in light, which is a hallmark of the circadian clock. Another such hallmark is the ability to maintain activity patterns established under L–D cycles after being transferred to constant darkness (Fig. 1a and Extended Data Fig. 1a, h).

Mutation of *cry* causes only subtle effects on circadian behaviour[3] (Extended Data Fig. 1b, h). Flies also show rhythmic behaviour after photoentrainment if they are missing the phospholipase C (PLC) NORPA[2,5], which is required for phototransduction in the compound eye, or if they are doubly mutant for *norpA* and *cry*[2,5] (Extended Data Fig. 1c, d, h). Phototransduction in Hofbauer–Buchner eyelet photoreceptors couples to Rh6 and the TRPL channel[7–9], but is independent of NORPA[5]. Flies triply mutant for *rh5, rh6* and *cry*[5], for *norpA*, *cry* and *trp*, or for *norpA*, *trpl* and *cry* are entrained by L–D cycles (Extended Data Fig. 1e–h). Thus, as proposed[5], there is likely to be an additional light input pathway that influences the circadian clock preceding exposure to D–D.

The *Drosophila* genome encodes an uncharacterized opsin, Rh7 (Extended Data Fig. 2a), which shares 27–30% amino acid identity with other opsins in *Drosophila melanogaster*. Rh7 is conserved in other *Drosophila* species (79–99% identity) and in *Aedes aegypti* and *Anopheles gambiae* (49–52% identity)[10]. Photoreceptor cells in the compound eye and ocelli express six opsins (Rh1–Rh6; Extended Data Fig. 2b, c). However, a mutation (gl^{60j}) that eliminates ocular photoreceptor cells and reduces levels of *rh1* (also known as *ninaE*)–*rh6* RNA did not reduce *rh7* RNA levels (Fig. 1b). We performed RNA sequencing (RNA-seq) using RNA from flies expressing a cell death gene (*GMR-hid*) in ocular photoreceptor cells. The numbers of *rh1*–*rh6* transcripts were reduced markedly, whereas the number of *rh7* transcripts was unchanged (Fig. 1c). We did not detect Rh7 in the compound eye with Rh7 antibodies (see below; Extended Data Fig. 2b–e). We generated an *rh7* null allele, $rh7^1$ (Extended Data Fig. 2f, g), and tested the light responses of $rh7^1$ mutant flies by performing electroretinogram (ERG) recordings. The ERGs of control and $rh7^1$ flies were indistinguishable (Extended Data Fig. 2h–j). Thus, Rh7 neither was expressed nor functioned in known photoreceptor cells.

To address whether Rh7 is a light receptor, we tested whether it could substitute for Rh1 in R1–6 photoreceptor cells. Expression of *rh7* rescued a wild-type-like ERG in the *rh1* mutant ($ninaE^{I17}$; Extended Data Fig. 2k–m). To assess the light response due to Rh7 only, we eliminated the light responses from the remaining two photoreceptor cells (R7 and R8), which express other rhodopsins. Phototransduction was abolished in $norpA^{P24}$ flies (Fig. 1d, e). We restored a photoresponse in R1–6 cells of $norpA^{P24}$ flies by expressing a $norpA^{+}$ transgene using the *rh1* promoter (*rh1>norpA*; Fig. 1f). When we eliminated *rh1* ($ninaE^{I17}$) from the $norpA^{P24}$;*rh1>norpA* flies, the flies were unresponsive to light (Fig. 1g). We restored a light response by expressing *rh7* in the R1–6 cells (*rh1>rh7*; Fig. 1h). Thus, Rh7 is a light sensor and is capable of coupling to a Gq–PLC signalling pathway. We expressed Rh7 in HEK293T cells and found that it responded to light with a peak at 397 nm (Fig. 1i, j).

We raised Rh7 antibodies, which stained two groups of cells in the brain, consistent with a subset of central pacemaker neurons (Fig. 2a and Extended Data Fig. 3a, c). The approximately 150 pacemaker neurons express Period (Per), a core component of the circadian clock[11–13], and are classified as dorsal and lateral neurons (Extended Data Fig. 3a). The 15–16 lateral neurons include 5–6 dorsal lateral neurons (LNds), 4–5 large ventrolateral neurons (l-LNvs), and 4–5 small ventrolateral neurons (s-LNvs)[14]. Rh7 and Per were co-expressed in the LNvs (Fig. 2a–c), which express the neuropeptide pigment dispersing factor (PDF)[15] (Fig. 2d–f). We also detected Rh7-positive neurons in the vicinity of dorsal neurons 1 (DN1s) (Extended Data Fig. 3a, c), half of which expressed *cry*[16] (Extended Data Fig. 3d, e). However, these neurons did not co-stain with the *cry* reporter (*cry-Gal4*.E13 (refs 2, 17); Extended Data Fig. 3e). We did not detect anti-Rh7 staining in other central pacemaker neurons or in $rh7^1$ flies (Fig. 2g–i and Extended Data Fig. 3b).

Cry mediates rapid increases in action potentials evoked by blue light (450 nm peak) in l-LNvs[18–20]. We compared the electrophysiological

[1]Neuroscience Research Institute and Department of Molecular, Cellular and Developmental Biology, University of California, Santa Barbara, Santa Barbara, California 93106, USA. [2]Department of Biological Chemistry, The Johns Hopkins University School of Medicine, Baltimore, Maryland 21205, USA. [3]Department of Physiology and Biophysics, University of California, Irvine, Irvine, California 92697, USA. [4]Center for Circadian Biology, University of California, San Diego, La Jolla, California 92093, USA.

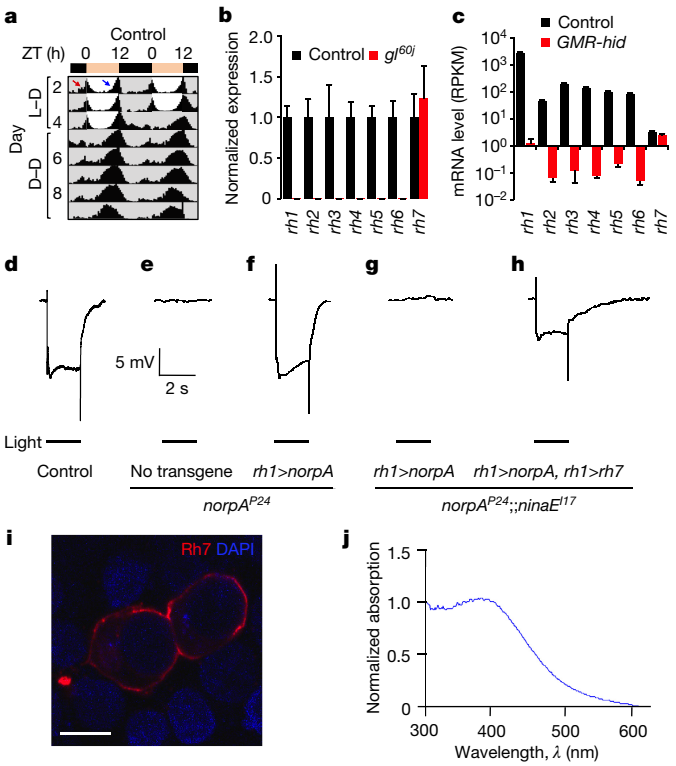

Figure 1 | Rh7 is a light receptor. a, Actogram obtained with control flies entrained under L–D cycles and released to constant darkness (D–D). Red and blue arrows indicate morning and evening anticipation, respectively. $n = 62$. **b**, Quantitative real-time PCR analysis of *opsin* genes using RNA from heads. Error bars indicate s.e.m. $n = 3$ per genotype. **c**, *Opsin* RNA-seq mRNA levels were quantified as reads per kilobase of transcript per million mapped reads (RPKM). Error bars indicate s.e.m. **d**–**h**, ERG responses using 2-s light. **d**, Control flies. **e**, $norpA^{P24}$ mutants. **f**, Expression of *norpA* using the *rh1* promoter (*rh1>norpA*) in a $norpA^{P24}$ background. **g**, Expression of *rh1>norpA* in a $norpA^{P24}$;;$ninaE^{I17}$ background. **h**, Expression of *rh1>norpA and UAS–rh7* under the control of the *rh1–Gal4* driver (*rh1>norpA* and *rh1>rh7*, respectively) in a $norpA^{P24}$;;$ninaE^{I17}$ background. **i**, HEK293T cells expressing Rh7 and stained with anti-Rh7. The DAPI stain indicates nuclei. Scale bar, 10 μm. **j**, Absorbance spectrum of Rh7 from HEK293T cells expressing Rh7.

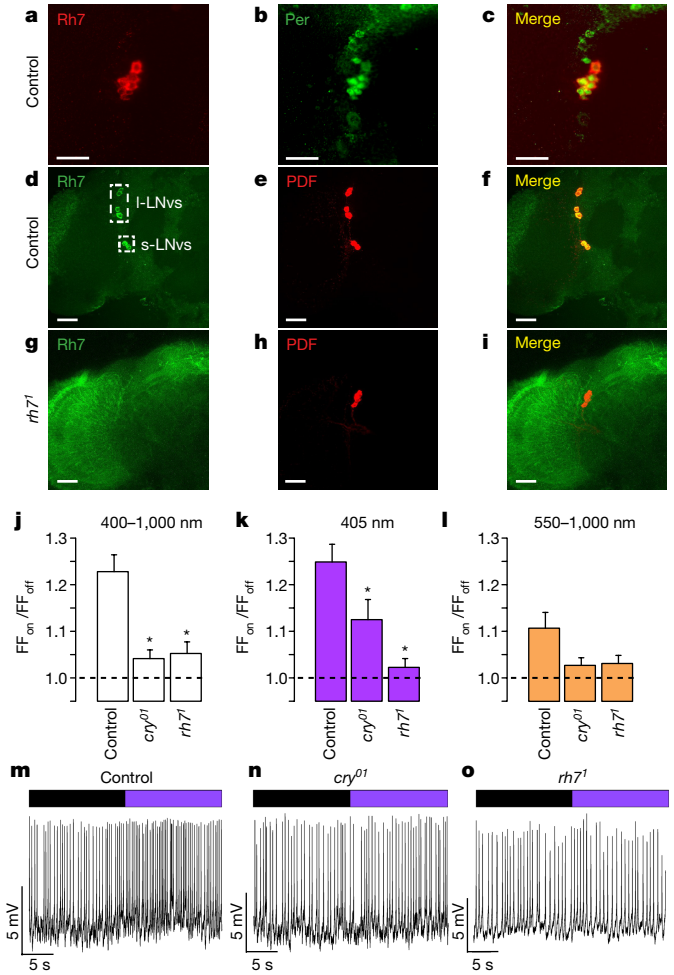

Figure 2 | Rh7 contributes to light sensitivity of circadian pacemaker neurons. a–**i**, Control and $rh7^1$ brains stained with the indicated antibodies. Merged images are on the right. Scale bars, 20 μm. **j**–**l**, Average firing frequencies of l-LNvs during 'lights on' relative to firing frequencies during 'lights off' (FF_{on}/FF_{off}). Error bars indicate s.e.m. $^*P < 0.05$. One-way ANOVA (Kruskal–Wallis test) followed by Dunn's test. **j**, White light. Control ($n = 74$), cry^{01} ($n = 80$, $P < 0.05$ versus control) and $rh7^1$ ($n = 60$, $P < 0.05$ versus control). **k**, 405 nm violet light. Control ($n = 76$), cry^{01} ($n = 89$, $P < 0.05$ versus control) and $rh7^1$ ($n = 66$, $P < 0.05$ versus control). **l**, Orange light. Control ($n = 58$), cry^{01} ($n = 65$) and $rh7^1$ ($n = 46$). **m**–**o**, Representative recordings showing responses of l-LNv neurons to 405 nm light. Purple bar, 405 nm light; black bar, no light.

responsiveness to white (400–1,000 nm) and violet (405 nm) light in control and $rh7^1$ l-LNvs. The l-LNv responses to white and violet light were greatly diminished in cry^{01} and $rh7^1$ flies (Fig. 2j, k, m–o). Control, cry^{01} and $rh7^1$ flies showed minimal or no response to orange light (550–1,000 nm; Fig. 2l).

To address the importance of Rh7 to entrainment, we first investigated its contribution to circadian phase changes in response to a nighttime light pulse, which shifts the phase of the clock[21]. The direction of the shift depends on when the light is presented[21–23]. Lights were turned on and off at Zeitgeber time (ZT)0 and ZT12, respectively. An early night light pulse (ZT14–18) produced a phase delay in controls, whereas a late night light pulse (ZT20–22) caused a phase advance[21] (Fig. 3a). As previously reported[3,22], cry^{01} flies displayed severely impaired phase shifting to early or late night pulses (Fig. 3a and Extended Data Fig. 4).

We exposed $rh7^1$ flies to nighttime light pulses. The phase delay was normal if the stimulus was presented early (ZT14; Fig. 3a and Extended Data Fig. 4). However if the light pulse occurred later, the degree of phase shift was significantly reduced (ZT16, $P < 0.01$; ZT18, $P < 0.01$; ZT20, $P < 0.01$; ZT22, $P < 0.01$; Fig. 3a and Extended Data Fig. 4). We knocked down *rh7* RNA in wild-type flies using an LNv-specific driver (*pdf–Gal4*) (Extended Data Fig. 3f–i) and then exposed the flies to light at ZT22. These flies exhibited the same phase advance defect as $rh7^1$ flies (Fig. 3b), indicating that Rh7 is required in PDF-positive neurons for normal photoentrainment.

Phase advances due to light pulses late at night (ZT22) correlate with light-induced degradation of the core clock protein Timeless (Tim)[24]. Tim degradation depends on binding to Cry[24], or results from neuronal activation[25]. As light-induced neuronal firing is reduced in $rh7^1$ flies, light-induced degradation of Tim might be impaired. To test this hypothesis, we applied a light pulse at ZT22 and assayed anti-Tim signals in PDF neurons (LNvs) 55 min later. In controls, light caused a 4.8-fold decline in Tim (Fig. 3c, f). However, in $rh7^1$ LNvs, light caused only a slight reduction in anti-Tim staining, which was not statistically significant (Fig. 3d, f). We rescued this defect with a genomic transgene (Fig. 3e, f).

Another test of photoentrainment is to assess the number of days required to adjust to a delay in the light-to-dark transition. If control flies are entrained under L–D cycles, and then the transition from light to darkness is delayed by 8 h, they quickly re-entrain to the new L–D cycle[1] (Fig. 3g, h). The evening peak shifts by 7.6 ± 0.1 h on day 1 and 7.9 ± 0.1 h on day 2 (Fig. 3g). Consistent with a previous study[1], cry^{01} flies shifted by only 4.6 ± 0.2 h on day 1 and 6.5 ± 0.1 h on day 2, and required 3 days to establish stable peak activity (Fig. 3g, i). We

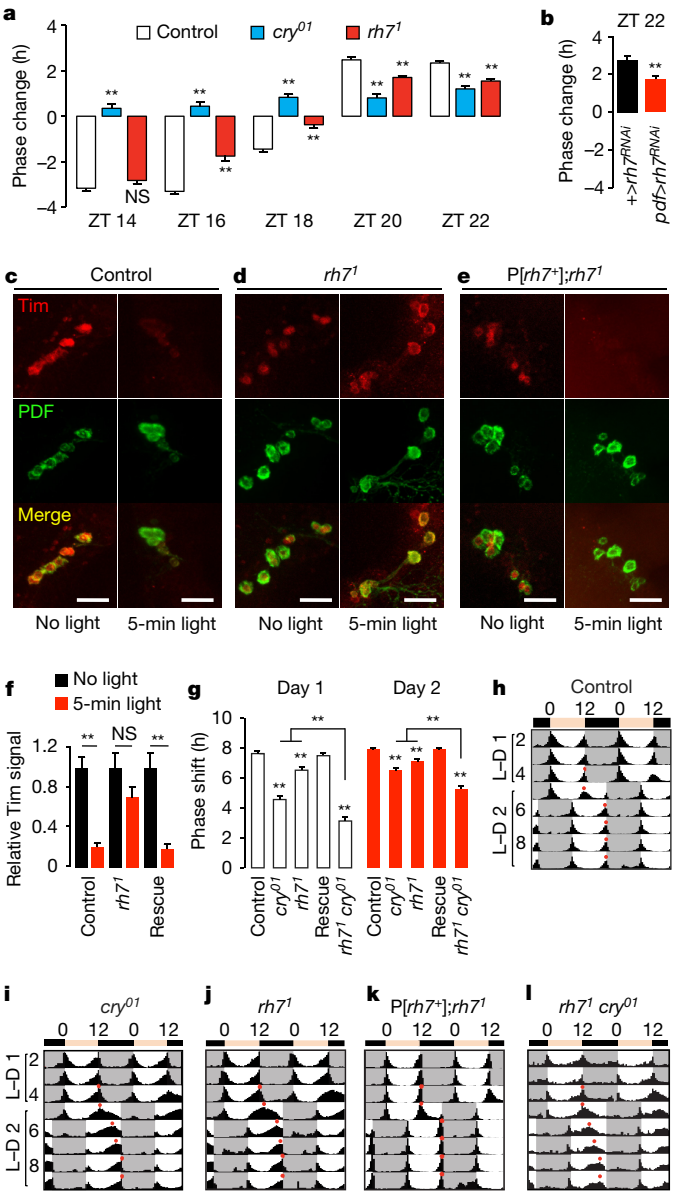

Figure 3 | Rh7 is a circadian light receptor. a, Phase response of flies to 5-min white light at the indicated ZT. Negative and positive phase changes indicate phase delays and phase advances, respectively. Three independent assays per genotype ($n = 8$–32 per experiment). Total flies tested: ZT14, control, $n = 56$; cry^{01}, $n = 46$; $rh7^{1}$, $n = 55$. ZT16, control, $n = 61$; cry^{01}, $n = 52$; $rh7^{1}$, $n = 57$. ZT18, control, $n = 61$; cry^{01}, $n = 51$; $rh7^{1}$, $n = 77$. ZT20, control, $n = 45$; cry^{01}, $n = 39$; $rh7^{1}$, $n = 48$. ZT22, control, $n = 54$; cry^{01}, $n = 60$; $rh7^{1}$, $n = 48$. NS, not significant. Error bars indicate s.e.m. * *$P < 0.01$. One-way ANOVA (Kruskal–Wallis test) followed by Dunn's test. **b**, Phase responses to 5-min white light stimulation at ZT22. Three independent assays per genotype ($n = 8$–24 per experiment). +>$rh7^{RNAi}$ (*UAS–rh7*^{RNAi}), $n = 40$; *pdf*>$rh7^{RNAi}$ (*UAS–rh7*^{RNAi} and *pdf–Gal4*), $n = 52$. * *$P < 0.01$, unpaired Student's *t*-test. **c**–**e**, Flies were exposed to 5-min light stimuli at ZT22, and the LNvs were stained with anti-Tim and anti-PDF at ZT23. Scale bars, 40 μm. **f**, Quantification of light-mediated degradation of Tim protein in LNvs. The rescue flies are P[$rh7^{+}$];$rh7^{1}$. Animals tested: control, dark $n = 6$, light $n = 4$; $rh7^{1}$, dark $n = 5$, light $n = 4$; rescue, dark $n = 5$, light $n = 4$. NS, not significant. Error bars indicate s.e.m. **$P < 0.01$, unpaired Student's *t*-test. **g**, Quantification of the phase shifts on days 1 and 2 after the 8-h phase delay. Three or four independent assays per genotype ($n = 10$–30 per experiment). Control, $n = 95$; cry^{01}, $n = 96$; $rh7^{1}$, $n = 68$; P[$rh7^{+}$];$rh7^{1}$, $n = 60$; $rh7^{1}$ cry^{01}, $n = 66$. Error bars indicate s.e.m. One-way ANOVA (Kruskal–Wallis test) followed by Dunn's test. **$P < 0.01$. **h**–**l**, Actograms. Flies were entrained under L–D cycles. On day 5, the day cycle was extended by 8 h. Red dots indicate evening peaks.

found that $rh7^{1}$ flies displayed significant delays in phase shift (day 1, 6.5 ± 0.2 h, $P < 0.01$; day 2, 7.1 ± 0.1 h, $P < 0.01$; Fig. 3g, j) consistent with a contribution of Rh7 to photoentrainment. We rescued the defect with an $rh7^{+}$ genomic transgene (Fig. 3g, k). The impairment in the phase-shift exhibited by $rh7^{1}$ cry^{01} double mutant flies (day 1, 3.1 ± 0.2 h; day 2, 5.3 ± 0.2 h) was more severe than those seen in the single mutants (Fig. 3g, l).

Constant light (L–L) leads to arrhythmic circadian behaviour in wild-type flies[6] (Fig. 4a, d). However, *cry* mutant flies remain rhythmic in constant light[6] (93.1%; Fig. 4d and Extended Data Fig. 5a). Under L–L conditions, 19.0% of $rh7^{1}$ flies are also rhythmic, and this phenotype is rescued by a wild-type $rh7^{+}$ transgene (Fig. 4b–d and Extended Data Fig. 5b).

Because phototransduction promotes signal amplification and sensitivity to low light, we tested the effects of lack of Rh7 on rhythmicity by photoentraining $rh7^{1}$ flies and then exposing them to constant dim light (10 lx). Few control flies maintained rhythmicity even under dim light, whereas all cry^{01} flies were rhythmic (Fig. 4e, h and Extended Data Fig. 5c). Notably, the majority of $rh7^{1}$ flies maintained rhythmicity under constant dim light (66.7%; Fig. 4f–h). We restored wild-type responses with an $rh7^{+}$ genomic transgene (Extended Data Fig. 5d). These data suggest that Rh7 is required for sensitizing the Cry-dependent circadian photoresponse under dim light conditions.

PDF-expressing LNvs promote light-dependent arousal[26,27]. To test whether Rh7 functions in arousal, we stimulated the flies at night (ZT22) with a 5-min white light pulse. The $rh7^{1}$ flies displayed decreased light-coincident arousal (Fig. 4i and Extended Data Fig. 5e) and a longer arousal delay than control flies (Extended Data Fig. 5f), and these defects were at least as great as those exhibited by cry^{01} flies[20] (Fig. 4i and Extended Data Fig. 5e, f). Responses to red light were not impaired significantly in the mutant flies (Extended Data Fig. 5g). The $rh7^{1}$ cry^{01} double mutant, but not the single mutants, exhibited a deficit in violet light arousal (405 nm; Extended Data Fig. 5h), indicating that the two light sensors compensate for each other during the arousal response.

We tested for a potential role of Rh7 in maintaining rhythmic behaviour during constant darkness (D–D) following L–D entrainment. The mutant flies showed rhythmic diurnal and circadian behaviour similar to that of wild-type flies (Fig. 4j, k, p). As previously shown[1], cry^{b} flies also photoentrained and exhibited rhythmic diurnal and circadian behaviour (Fig. 4l, p). However, $rh7^{1}$ cry^{b} double mutant flies showed profound deficits. Over one-third (37.2%) of the animals were arrhythmic (Fig. 4m, p), possibly owing to insufficient synchronization of the molecular clock between different groups of central pacemaker neurons in the absence of both light sensors intrinsic to these cells. The remaining rhythmic flies displayed much longer periodicity during D–D than did controls (control, 23.8 ± 0.08 h; $rh7^{1}$ cry^{b}, 27.3 ± 0.07 h, $P < 0.01$; Fig. 4j, n). $rh7^{1}$ cry^{01} double mutants displayed similar impairments (Extended Data Fig. 6a–c). Thus, at least one of the two light receptors is required in pacemaker neurons for normal rhythmic behaviour. We rescued these defects with an $rh7^{+}$ genomic transgene (Fig. 4o, p).

Although flies with single gl^{60j}, $rh7^{1}$ or *cry* mutations display photoentrainment impairments[1], they are capable of circadian rhythmicity. Thus, any two of these three photoreceptors (Cry, Rh7 and *gl*-dependent) are sufficient for rhythmic circadian behaviour. However, Rh7 is insufficient on its own because gl^{60j} cry^{b} flies are circadian blind[1]. To test whether *cry* alone is sufficient for rhythmic behaviour, we subjected the $rh7^{1}$ gl^{60j} double mutant flies to a L–D regime followed by D–D, and found that 25% were arrhythmic (Extended Data Fig. 6d–h). Thus, although Cry alone cannot preserve fully wild-type circadian behaviour, it enables flies to maintain greater rhythmicity than just Rh7 or *gl*-dependent photoreceptor cells. We exposed $rh7^{1}$ gl^{60j} flies to a 5-min light pulse at ZT22 to test their circadian phase-response. Although $rh7^{1}$ and gl^{60j} single mutants showed a decreased phase-advance, $rh7^{1}$ gl^{60j} double mutant flies displayed a greater impairment (Extended

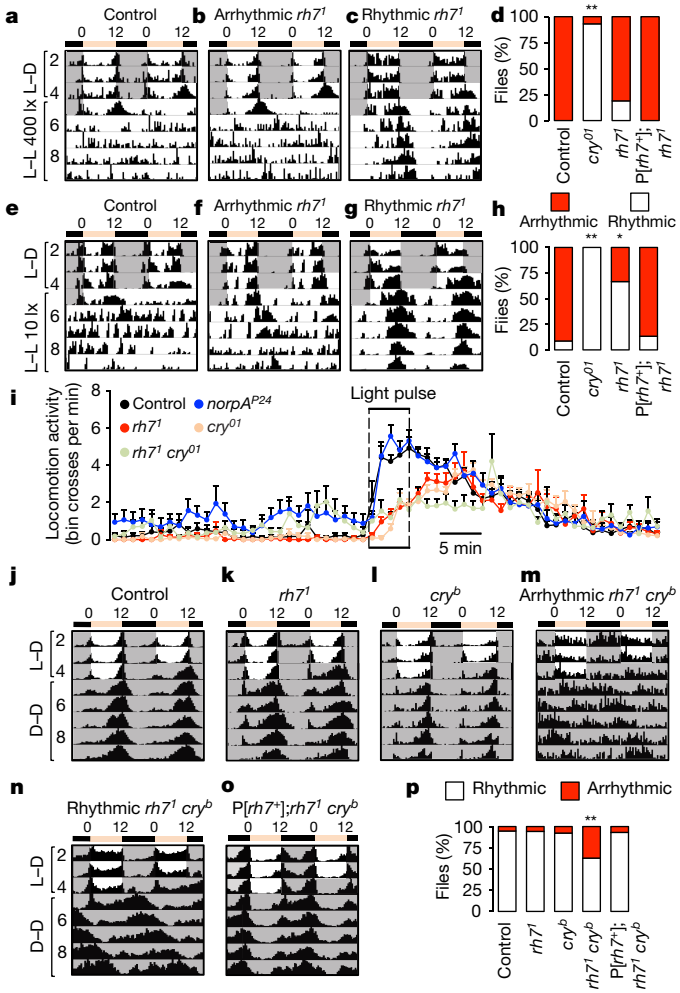

Figure 4 | Effects of *rh7* mutation on circadian behaviour in response to constant light or constant darkness and on arousal in response to a light pulse. a–c, Actograms showing circadian responses of flies entrained to L–D cycles and released to constant light (L–L) of ~400 lx. **d**, Percentages of rhythmic and arrhythmic flies. Fisher's exact test. $^{**}P < 0.01$. Control, $n = 48$; cry^{01}, $n = 29$; $rh7^1$, $n = 58$; P[$rh7^+$];$rh7^1$, $n = 16$. **e–g**, Actograms showing circadian responses of flies entrained under L–D cycles and released to dim L–L of ~10 lx. **h**, Percentages of rhythmic and arrhythmic flies. Fisher's exact test. $^{*}P < 0.05$. $^{**}P < 0.01$. Control, $n = 23$; cry^{01}, $n = 30$; $rh7^1$, $n = 27$; P[$rh7^+$];$rh7^1$, $n = 15$. **i**, Light-dependent arousal impaired by the $rh7^1$ mutation. Average locomotion activities (bin crosses per min) at ZT22. The box indicates the 5-min white light pulse. Error bars indicate s.e.m. **j–o**, Average actograms showing synergistic effect of the cry^b and $rh7^1$ mutations on circadian behaviour. The flies were entrained to L–D cycles and released to constant darkness. $rh7^+$ genomic transgene, P[$rh7^+$]. **p**, Percentages of rhythmic and arrhythmic flies. $^{**}P < 0.01$. Fisher's exact test. Control, $n = 76$; $rh7^1$, $n = 29$; cry^b, $n = 39$; $rh7^1$ cry^b, $n = 78$; P[$rh7^+$];$rh7^1$ cry^b, $n = 29$.

Data Fig. 6i). As cry^{01} flies also showed defects in the phase-response to a 5-min pulse (Fig. 3a), multiple light-input pathways contribute to circadian light sensation.

To test whether *rh7* functions in LNvs neurons, we performed rescue experiments. Expression of *rh7* (*UAS–rh7*) using either the *tim–GAL4* driver or the *pdf–GAL4* driver rescued the increase in arrhythmicity exhibited by $rh7^1$ cry^b flies (Extended Data Fig. 7). Introduction of other rhodopsins into PDF-positive neurons also restored normal rhythmicity (Extended Data Fig. 8), further supporting a rhodopsin-based mechanism for circadian function in LNvs.

In s-LNvs and l-LNvs, Per protein peaks during dawn (ZT22–ZT2) and enters a trough[28] (Extended Data Fig. 9a–c). In $rh7^1$ flies, Per also displayed oscillations in LNvs (Extended Data Fig. 9d–f), consistent with their rhythmic behaviour under L–D cycles. Per oscillations in LNvs are altered in cry^b mutants[1,3]. The trough and peak are delayed in s-LNvs, and there is a large reduction in oscillation amplitude in l-LNvs (Extended Data Fig. 9g–i). In $rh7^1$ cry^b flies, Per levels remained high from ZT2 to ZT14 in s-LNvs and peaked shortly after dusk (ZT14) in l-LNvs (Extended Data Fig. 9j–l). PDF does not oscillate in control[29] or $rh7^1$ LNvs (Extended Data Fig. 9a, d).

In the eye, rhodopsins signal through the PLC encoded by *norpA*. However, *norpA* and *cry* double mutant flies exhibit normal rhythmicity during constant darkness following L–D entrainment[2,5] (Extended Data Fig. 1d, h), indicating that Rh7 signalling in LNvs is NORPA-independent. To investigate whether the other PLCβ (PLC21C) functions in PDF neurons, we combined two *UAS–plc21C* RNAi lines with the *pdf–Gal4* driver (Extended Data Fig. 10a), and then exposed the flies to a white-light pulse for 5 min at ZT22. Knockdown of *plc21C* caused reductions in phase-advance at ZT22 (Extended Data Fig. 10b–g), similar to the effects of the $rh7^1$ mutation (Fig. 3a).

In summary, our work establishes a role for a rhodopsin in the central brain. Rh7 is strategically expressed in PDF-positive cells, which appear to be master light input clock neurons that also receive input from the optical lobes[26]. The fact that PDF-positive neurons express two distinct light sensors (Rh7 and Cry) highlights their key role in circadian photoentrainment. In the mammalian retina, around 1% of retinal ganglion cells are intrinsically photosensitive (ipRGCs), and these cells function in circadian photoentrainment. ipRGCs are directly light sensitive owing to the expression of melanopsin and also receive light information from rods and cones. The striking similarities between *Drosophila* PDF-positive neurons and ipRGCs indicate a common strategy for circadian photoentrainment. Opsins are also expressed in the mammalian brain[30], although their functions are unknown. Because light penetrates the mammalian skull, our findings raise the possibility that neurons in the mammalian brain also sense light and contribute to photoentrainment of circadian rhythms.

Online Content Methods, along with any additional Extended Data display items and Source Data, are available in the online version of the paper; references unique to these sections appear only in the online paper.

Received 24 June 2016; accepted 30 March 2017.
Published online 10 May 2017.

1. Helfrich-Förster, C., Winter, C., Hofbauer, A., Hall, J. C. & Stanewsky, R. The circadian clock of fruit flies is blind after elimination of all known photoreceptors. *Neuron* **30,** 249–261 (2001).
2. Emery, P. *et al.* *Drosophila* CRY is a deep brain circadian photoreceptor. *Neuron* **26,** 493–504 (2000).
3. Stanewsky, R. *et al.* The cry^b mutation identifies cryptochrome as a circadian photoreceptor in *Drosophila*. *Cell* **95,** 681–692 (1998).
4. Ozturk, N., Selby, C. P., Annayev, Y., Zhong, D. & Sancar, A. Reaction mechanism of *Drosophila* cryptochrome. *Proc. Natl Acad. Sci. USA* **108,** 516–521 (2011).
5. Szular, J. *et al.* *Rhodopsin 5-* and *Rhodopsin 6*-mediated clock synchronization in *Drosophila melanogaster* is independent of retinal phospholipase C-β signaling. *J. Biol. Rhythms* **27,** 25–36 (2012).
6. Emery, P., Stanewsky, R., Hall, J. C. & Rosbash, M. A unique circadian-rhythm photoreceptor. *Nature* **404,** 456–457 (2000).
7. Helfrich-Förster, C. *et al.* The extraretinal eyelet of *Drosophila*: development, ultrastructure, and putative circadian function. *J. Neurosci.* **22,** 9255–9266 (2002).
8. Malpel, S., Klarsfeld, A. & Rouyer, F. Larval optic nerve and adult extra-retinal photoreceptors sequentially associate with clock neurons during *Drosophila* brain development. *Development* **129,** 1443–1453 (2002).
9. Sprecher, S. G. & Desplan, C. Switch of *Rhodopsin* expression in terminally differentiated *Drosophila* sensory neurons. *Nature* **454,** 533–537 (2008).
10. Senthilan, P. R. & Helfrich-Förster, C. Rhodopsin 7—the unusual Rhodopsin in *Drosophila*. *PeerJ* **4,** e2427 (2016).
11. Zerr, D. M., Hall, J. C., Rosbash, M. & Siwicki, K. K. Circadian fluctuations of *period* protein immunoreactivity in the CNS and the visual system of *Drosophila*. *J. Neurosci.* **10,** 2749–2762 (1990).
12. Kaneko, M. & Hall, J. C. Neuroanatomy of cells expressing clock genes in *Drosophila*: transgenic manipulation of the *period* and *timeless* genes to mark the perikarya of circadian pacemaker neurons and their projections. *J. Comp. Neurol.* **422,** 66–94 (2000).
13. Konopka, R. J. & Benzer, S. Clock mutants of *Drosophila melanogaster*. *Proc. Natl Acad. Sci. USA* **68,** 2112–2116 (1971).

14. Helfrich-Förster, C. Robust circadian rhythmicity of *Drosophila melanogaster* requires the presence of lateral neurons: a brain-behavioral study of *disconnected* mutants. *J. Comp. Physiol. A* **182,** 435–453 (1998).
15. Renn, S. C., Park, J. H., Rosbash, M., Hall, J. C. & Taghert, P. H. A *pdf* neuropeptide gene mutation and ablation of PDF neurons each cause severe abnormalities of behavioral circadian rhythms in *Drosophila*. *Cell* **99,** 791–802 (1999).
16. Yoshii, T., Todo, T., Wülbeck, C., Stanewsky, R. & Helfrich-Förster, C. Cryptochrome is present in the compound eyes and a subset of *Drosophila*'s clock neurons. *J. Comp. Neurol.* **508,** 952–966 (2008).
17. Helfrich-Förster, C. *et al.* Development and morphology of the clock-gene-expressing lateral neurons of *Drosophila melanogaster*. *J. Comp. Neurol.* **500,** 47–70 (2007).
18. Fogle, K. J., Parson, K. G., Dahm, N. A. & Holmes, T. C. CRYPTOCHROME is a blue-light sensor that regulates neuronal firing rate. *Science* **331,** 1409–1413 (2011).
19. Sheeba, V., Gu, H., Sharma, V. K., O'Dowd, D. K. & Holmes, T. C. Circadian- and light-dependent regulation of resting membrane potential and spontaneous action potential firing of *Drosophila* circadian pacemaker neurons. *J. Neurophysiol.* **99,** 976–988 (2008).
20. Fogle, K. J. *et al.* CRYPTOCHROME-mediated phototransduction by modulation of the potassium ion channel β-subunit redox sensor. *Proc. Natl Acad. Sci. USA* **112,** 2245–2250 (2015).
21. Dushay, M. S. *et al.* Phenotypic and genetic analysis of *Clock*, a new circadian rhythm mutant in *Drosophila melanogaster*. *Genetics* **125,** 557–578 (1990).
22. Kistenpfennig, C., Hirsh, J., Yoshii, T. & Helfrich-Förster, C. Phase-shifting the fruit fly clock without cryptochrome. *J. Biol. Rhythms* **27,** 117–125 (2012).
23. Vinayak, P. *et al.* Exquisite light sensitivity of *Drosophila melanogaster* cryptochrome. *PLoS Genet.* **9,** e1003615 (2013).
24. Koh, K., Zheng, X. & Sehgal, A. JETLAG resets the *Drosophila* circadian clock by promoting light-induced degradation of TIMELESS. *Science* **312,** 1809–1812 (2006).
25. Guo, F., Cerullo, I., Chen, X. & Rosbash, M. PDF neuron firing phase-shifts key circadian activity neurons in *Drosophila*. *eLife* **3,** e02780 (2014).
26. Sheeba, V. *et al.* Large ventral lateral neurons modulate arousal and sleep in *Drosophila*. *Curr. Biol.* **18,** 1537–1545 (2008).
27. Shang, Y., Griffith, L. C. & Rosbash, M. Light-arousal and circadian photoreception circuits intersect at the large PDF cells of the *Drosophila* brain. *Proc. Natl Acad. Sci. USA* **105,** 19587–19594 (2008).
28. Siwicki, K. K., Eastman, C., Petersen, G., Rosbash, M. & Hall, J. C. Antibodies to the *period* gene product of *Drosophila* reveal diverse tissue distribution and rhythmic changes in the visual system. *Neuron* **1,** 141–150 (1988).
29. Nitabach, M. N. *et al.* Electrical hyperexcitation of lateral ventral pacemaker neurons desynchronizes downstream circadian oscillators in the fly circadian circuit and induces multiple behavioral periods. *J. Neurosci.* **26,** 479–489 (2006).
30. Blackshaw, S. & Snyder, S. H. Encephalopsin: a novel mammalian extraretinal opsin discretely localized in the brain. *J. Neurosci.* **19,** 3681–3690 (1999).

Supplementary Information is available in the online version of the paper.

Acknowledgements We thank A. Sehgal, M. Rosbash, M. Wu and P. Emery for fly stocks; A. Sehgal and S. Britt for antibodies; and E. Guzman, H. Zhou and the Next Generation Sequencing Core at the UCSB Biological Nanostructures Laboratory for help with the RNA-seq. This work was supported by grants to C.M. from the National Eye Institute (EY008117) and the National Institute on Deafness and other Communication Disorders (DC007864), and to T.C.H. from National Institute of General Medical Sciences (GM102965 and GM107405).

Author Contributions J.D.N., T.C.H. and C.M. designed the study. J.D.N. and L.S.B. performed experiments, and all authors analysed the data. J.D.N. and C.M. wrote the manuscript with input from T.C.H. and L.S.B.

Author Information Reprints and permissions information is available at www.nature.com/reprints. The authors declare no competing financial interests. Readers are welcome to comment on the online version of the paper. Publisher's note: Springer Nature remains neutral with regard to jurisdictional claims in published maps and institutional affiliations. Correspondence and requests for materials should be addressed to C.M. (craig.montell@lifesci.ucsb.edu).

Reviewer Information *Nature* thanks C. Desplan, R. Stanewsky and the other anonymous reviewer(s) for their contribution to the peer review of this work.

METHODS

No statistical methods were used to predetermine sample sizes. All behaviour data were collected in a random manner. No blinding method was used in assessing experimental outcomes.

Fly stocks. The following flies were obtained from Bloomington Stock Center: isogenized w^{1118} (BL5905), $norpA^{P24}$ (BL9048), *ninaE-norpA* (*rh1>norpA*; this is a direct fusion of the *ninaE* promoter to the *norpA* coding region; BL52276), *ninaE–Gal4* (*rh1–Gal4*; BL8691), trp^{MB} (BL23636), $trpl^{MB}$ (BL29314), *UAS–mcherry-NLS* (BL38425), gl^{60j} (BL 509), *pdf–Gal4* (BL6900), and two *UAS–plc21C* RNAi lines (01210, BL 31269 and 01211, BL31270). *GMR–hid*[31] was obtained from the *Drosophila* Genetic Resource Center, Kyoto (108419). We used w^{1118} as the control strain. The *UAS–rh7* RNAi line (v1478) was from VDRC Stock Center. The *tim–Gal4* transgene[32] was provided by A. Sehgal. The *cry–Gal4.E13* transgene[2] was from M. Rosbash. The cry^{b} and cry^{01} flies[2,33] were provided by M. Wu and the $rh5^{02}$, $rh6^{01}$, *UAS-rh3*, *UAS-rh4* and *UAS-rh5* lines[34,35] were provided by C. Desplan. We also used $ninaE^{I17}$ flies[36].

Cloning of the *rh7* cDNA and generation of transgenic flies. To clone the *rh7* coding region, we prepared mRNA from w^{1118} heads, performed reverse transcription (RT)-PCR using the following primers, and cloned the cDNA into the TOPO vector (pCR2.1-TOPO, Invitrogen). Primers: *rh7* forward, GCGGCCGCCACCATGGAGGCCATCATCATGACG; *rh7* reverse, GCGGCCGCTCAGAACTTACTCTGTTCCATGAC. To generate the *UAS–rh7* transgene, we subcloned the *rh7* open reading frame into the NotI site of the pUAST vector. To construct the plasmid for expression of Rh7 in HEK293T cells, we subcloned the *rh7* open reading frame between the BamH1 and Xba1 sites of the pCS2+MT vector using the following primers: *rh7* forward, ATCAGATCTCACCATGGAGGCCATCATCATGACG; *rh7* reverse, ATCTCTAGATCAGAACTTACTCTGTTCCATGAC.

To generate transgenic flies expressing an Rh7–FLAG fusion protein, we first constructed the pUAST–FLAG vector using the following two oligonucleotides, which we annealed and cloned into the XhoI and XbaI sites of the pUAST vector: FLAG 5′-XbaI, TCGAGGGGATTACAAGGATGACGACGATAAGTAAT and FLAG 3′-XhoI, CTAGATTACTTATCGTCGTCATCCTTGTAATCCCC. We amplified the *rh7* coding region using the same forward primer as above, in conjunction with the following reverse primer to eliminate the stop codon: *rh7* reverse$^{no\text{-}stop}$, GCGGCCGCGAACTTACTCTGTTCCATGAC. Both the *UAS–rh7* and *UAS–rh7–FLAG* transgenic flies were obtained by germline transformation using w^{1118} embryos (Bestgene Inc.).

To generate flies expressing an $rh7^{+}$ genomic transgene (P[$rh7^{+}$]), a BAC genomic DNA clone (CH322180G19) was obtained from the P[*acman*] collection[37]. The germline transformation took advantage of site-specific integration using the Φ31-attB/attP system (Bestgene Inc.).

Generation of $rh7^{1}$ mutant flies by homologous recombination. We produced the plasmid for knocking out *rh7* by ends-out homologous recombination[38] as follows. We PCR amplified two homologous arms (left, 3.2 kb and right, 3.3 kb) using the following primers: left arm forward, AATTGCTGGGATCCCTCAATTGGCCTAATCGGTTTCTG; left arm reverse, AATTGCTGGGTACCGACTGACTTGGCCAAATATTTACG; right arm forward, AATGCTGGCGGCCGCTTAAAATGCTGCCCGAGACT; right arm reverse, AATTGCTGGCGGCCGCTGGCTTATGAAGTTGCAAAAAG. We cloned the two arms into the targeting vector, pw35*loxp–Gal4*. This construct was designed to delete 540 base pairs (bp) 3′ to the *rh7* translational start site, and was replaced with a cassette containing the *mini-white* marker and *Gal4* flanked by two *loxP* sites. The upstream *loxP* sequence contained a translational start site that rendered the *Gal4* coding region out of frame. Consequently, the *Gal4* was not functional. To obtain the donor lines for generating the *rh7* knockout ($rh7^{1}$ allele), the targeting vector was injected into w^{1118} embryos (Bestgene Inc.). We mobilized the donor insertion by crossing the donor line to *y,w;P[70FLP]11* P[*70I-SceI*]*2B* noc^{Sco}/CyO flies (Bloomington Stock Center, BL6934). The progeny were screened for gene targeting in the *rh7* locus by PCR using two pairs of primers. The first pair (P1 and P2) were the following two primers that annealed to the first and second coding exons, and produced a DNA product (885 bp) only in the wild-type (Extended Data Fig. 2g): P1, CTCTCGCTCTCCGAGATGTT and P2, ACCACCGAAATCAGGCAATA. The following second pair of primers (P3 and P4) annealed to the *mini-white* gene and to a sequence 3′ to *rh7*, and therefore only generated a product in the $rh7^{1}$ mutant (4.4 kb; Extended Data Fig. 2g): P3, TGTACATAAAAGCGAACCGAACCT and P4, ACTGTGCGACAGAGTGAGAGAGCAATAGTA. After generating $rh7^{1}$, we outcrossed the flies to the control stain (w^{1118}) for five generations.

Genotyping *timeless*, *jetlag* and *period* alleles. To determine whether the key fly lines used in this study harboured the per^{SLIH}, tim^{ls} or jet^{c} mutations in the genetic background, we performed DNA sequencing. We extracted genomic DNA from adult flies, and amplified the relevant regions in the *per*, *tim* and *jet* genes by PCR (Phusion High-Fidelity DNA Polymerase, NEB) using the following primers: *per*: forward, GTCCACACACAACACCAAGG; reverse, TTGATGATCATGTCGCTGCT. *tim*: forward, TGGCTGGGGATTGAAAATAA; reverse, TTACAGATACCGCGCAAATG. *jet*: forward, AGCCGATCATAGTGGAGTGC; reverse, AAGGCACGCACAGGTTTACT.

We purified the PCR products and subjected them to DNA sequencing (DNA Sequencing Facility at the University of California, Berkeley). The per^{SLIH} allele has a C to A transversion at nucleotide 2688438. The control (per^{+}) sequence encompassing this region (2688436–2688448, *Drosophila* genome release r6.14) is CTCCGGCAGCAGT. The per^{SLIH} sequence is CTACGGCAGCAGT. All of the fly lines checked had sequences that matched per^{+}. These include: (1) $rh7^{1}$, (2) $rh7^{1}$ cry^{b}, (3) $rh7^{1}$ cry^{01}, (4) *pdf–Gal4* and (5) *rh7-RNAi*. The tim^{ls} allele has a single nucleotide insertion (C) after nucleotide 3504474 relative to tim^{s}. The sequence spanning this region in the control (tim^{ls}) is ATCAAAGTTCTGAT (3504473–3504486, *Drosophila* genome release r6.14) and in tim^{s} is ATAAAGTTCTGAT. We sequenced the following lines, all which had sequences that matched the control (tim^{s}): (1) cry^{01}, (2) $rh7^{1}$ and (3) P[$rh7^{+}$]; $rh7^{1}$. The jet^{c} allele has a T-to-A transversion at nucleotide 4949048. The control (jet^{+}) sequence spanning this region (4949059–4949047, *Drosophila* genome release r6.14) is CTTGATTATCTTC, while the jet^{c} sequence is CTTGATTATCTAC. We sequenced the following lines, all of which had sequences that matched the control (jet^{+}): (1) cry^{01}, (2) $rh7^{1}$ and (3) P[$rh7^{+}$];$rh7^{1}$.

Quantitative RT–PCR and RNA-seq data for opsins. To quantify expression of *opsin* genes (Fig. 1b), we isolated total RNA from ~50 fly heads from each of the indicated fly stocks, and used 1 μg total RNA from each sample as a template for reverse transcription using SuperScript III Reverse Transcriptase (ThermoFisher, cat. 18080093). Oligo dT primers were used for cDNA synthesis. cDNA preparation was subjected to real-time quantitative PCR (Roche, LightCycler 480 system) according to the LightCycler 480 SYBR Green 1 Master Mix (cat. 04707516001) protocol. The primers used for real-time quantitative PCR were: *rh1*: forward CGCTACCAAGTGATCGTCAA, reverse GTATGAGCGTGGGTTCCAGT. *rh2*: forward TCCGTGCTGGACAATGTG, reverse AATCATGCACATGGACCAGA. *rh3*: forward CGAGCAAAAGAACAGGAAGC, reverse TCGATACGCGACTCTTTGTG. *rh4*: forward GTAGCCCTCTGGCACGAAT, reverse TCTTCAGCACATCCAAGTCG. *rh5*: forward TCCTGACCACCTGCTCCTTC, reverse GCTCCAGCTCCAGACGATAC. *rh6*: forward CAAGGACTGGTGGAACAGGT, reverse GTACTTCGGGTGGCTCAATC. *rh7*: forward GTTTCCACGGGTCTGACAAT, reverse GCTGTAGCACCAGATCAGCA. *rp49*: forward GACGCTTCAAGGGACAGTATCTG, reverse AAACGCGGTTCTGCATGAG.

We also analysed *opsin* gene expression using an RNA-seq dataset (Fig. 1c). For each genotype, three independent RNA libraries were prepared from ~50 heads using the TruSeq Stranded mRNA Library Prep Kit. Pair-end sequencing was performed using the TruSeq platform (Illumina). Details of the RNA-seq experiments and data analysis will be presented elsewhere (J.D.N., I. Tekin and C.M., in preparation). *Opsin* RNA-seq mRNA levels were quantified as RPKM. RPKMs for each *opsin* were calculated independently and the average RPKMs are plotted.

Quantitative RT–PCR following *plc21C* RNAi knockdown. To knock-down *plc21C* expression, we combined each *UAS–plc21C* RNAi transgene (01210 and 01211) with *UAS–Dicer2*;;*actin–Gal4*. To quantify the efficacy of the RNAi, we extracted total RNA from ten adult flies (five male and five female), and used 1 μg total RNA from each sample as a template for reverse transcription using SuperScript III Reverse Transcriptase (ThermoFisher, cat. 18080093). Oligo dT primers were used for cDNA synthesis. cDNA preparation was subjected to quantitative PCR (Roche, LightCycler 480 system) according to the LightCycler 480 SYBR Green 1 Master Mix (cat. 04707516001) protocol. The *plc21C* primers used were: forward, GGATCTCTCCAAGTCGTTCG; reverse, TAGCCGCTTCACCAGCTTAT. The *rp49* primers were: forward, GACGCTTCAAGGGACAGTATCTG; reverse, AAACGCGGTTCTGCATGAG. In each reaction, we normalized expression of *plc21C* transcripts to *rp49*.

Generation of Rh7 antibodies. To obtain Rh7 antibodies, we generated a GST–Rh7 fusion protein by subcloning the region encoding the N-terminal 80 amino acids into the pGEX6P-1 vector (GE Healthcare Life Science). We expressed the fusion protein in *Escherichia coli* (BL21), purified the recombinant protein using glutathione sepharose beads (GE Healthcare Life Science) and generated antiserum in a rabbit (Covance). We affinity purified the antibodies by conjugating the antigen to Affi-Gel 10 (Bio-Rad).

Immunohistochemistry on whole mounts of *Drosophila* brains. We performed immunohistochemistry using whole-mounted fly brains as described previously[39]. Briefly, we fixed dissected brains for 15–20 min at 4 °C in 4% paraformaldehyde in phosphate buffer (0.1 M Na_3PO_4, pH 7.4) with 0.3% Triton-X100 (Sigma), hereafter referred to as PBT. The brains were blocked with 5% normal goat serum (Sigma) in phosphate buffer for 1 h at 4 °C. We then incubated the tissue with primary

antibodies at 4 °C for ≥24 h. After three washes in PBT, the brains were incubated overnight at 4 °C with the following secondary antibodies from Life Technologies: anti-mouse Alexa Fluor 488 or 568 Dyes, anti-rabbit Alexa Fluor 488 or 568 Dyes or Alexa dyes. The brains were washed three times with PBT and mounted in VECTASHIELD mounting medium (Vector Labs) for imaging. For Rh7 and PDF co-staining (Fig. 2d–i), four brains were examined.

Immunohistochemistry for circadian clock proteins (Tim and Per). To analyse light-mediated degradation of Tim (Fig. 3c–f), we entrained the flies for 3 days under 12 h light–12 h dark cycles (~600 lx LED white light). The flies were then exposed to a 5-min LED light stimulation (~600 lx) at ZT22, kept in the dark for 55 min, fixed at ZT23 under a red photographic safety light (for 45 min), and dissected for whole-mount immunostaining. Flies that were not exposed to the nocturnal light treatment were fixed and stained at the same time.

To examine Per staining at different ZT points (Extended Data Fig. 9), flies were entrained for 4 days under 12 h light (~400 lx)–12 h dark cycles, and were collected at the indicated ZTs. For nighttime samples, we handled the flies under a red photographic safety light. We prefixed whole flies at 4 °C with 4% paraformaldehyde in PBT for 45 min before dissecting out the brains. After the dissections, the brains were fixed again for 15–20 min at 4 °C in 4% paraformaldehyde in PBT.

We used the following primary antibodies: anti-Rh7 (1:250, rabbit), anti-Per (1:1,000, guinea pig), anti-Tim (1:1,000, rat)[40], anti-PDF (1:1,000, c7 mouse monoclonal antibody from the Developmental Studies Hybridoma Bank), anti-dsRed (1:500, mouse, Clontech Catalog #632392). The Per and Tim antibodies were contributed by A. Sehgal. The secondary antibodies (Thermo Fisher Scientific) were anti-rat Alexa Fluor 568 Dye and anti-guinea pig Alexa Fluor 555 Dye. We acquired the images using a Zeiss LSM 700 confocal microscope.

Immunostaining of whole-mounts of the *Drosophila* retina. To perform whole-mount staining of the retina, we dissected the retina (within the eye cup) and fixed the tissue at 4 °C in 4% paraformaldehyde in PBT for 20 min. After washing briefly in PBT, we blocked the retina for 1 h in PBT plus with 5% normal goat serum. We used the following primary antibodies: anti-Rh7 (1:250, rabbit), anti-Rh3 (1:200, mouse, gift from S. Britt, University of Colorado, Denver) and anti-Rh5 (1:200, mouse, gift from S. Britt, University of Colorado, Denver). The secondary antibodies were: anti-rabbit Alexa Fluor 568 Dye (1:1000) and anti-mouse Alexa Fluor 488 Dye (1:1000).

Circadian behaviour to assess rhythmicity and periodicity. Circadian experiments were performed at 25 °C using the *Drosophila* Activity Monitoring (DAM) System (Trikinetics). Individual 3–7-day-old male flies were loaded into monitoring tubes, which contained 1% agarose (Invitrogen) and 5% sucrose (Sigma) as the food source. The flies were entrained to 12 h light–12 h dark cycles for 4 days and released to constant darkness or constant light (10 lx for dim light conditions and 400 lx for bright light conditions, unless indicated otherwise) for at least six days to measure periodicity.

Data collection and analyses were performed using Clocklab (Actimetrics). Activity data for each fly were binned every 30 min for the circadian analyses. To obtain the periodicities, data from constant darkness were subjected to χ^2 periodograms and fast Fourier transfer analysis using Clocklab software. The rhythm strength of a fly was measured as the power minus the significance ($p-s$). Flies were considered arrhythmic based on either $p-s<10$ or FFT <0.03. Actograms of weakly rhythmic flies were visually inspected to confirm rhythmicity.

Circadian behaviour to assess light-mediated phase shift and phase delay. To investigate the effects on activity of 5-min light pulses at night (Fig. 3a, b; Extended Data Figs 4, 10), we first entrained the flies for 3 days under 12 h light–12 h dark cycles (~600 lx LED white light). During the night of the fourth L–D cycle (at ZT14, ZT16, ZT18, ZT20 or ZT22), we exposed the flies to a single 5-min light pulse (LED white light, ~600 lx), and then maintained the flies under constant darkness. The phase shift was calculated as the phase difference of the evening peaks before and after the light pulse. Negative and positive phase changes indicate phase delays and phase advances, respectively.

To conduct the phase delay experiments (Fig. 3g–l), we first entrained the flies for 4 days under 12 h light–12 h dark cycles (~400 lx LED white light). To obtain a phase delay of 8 h, on day 5 we extended the light phase to 20 h, and then returned the flies to normal 12 h dark–12 h light cycles. The phase shift magnitude was calculated as the phase difference between the evening peak of the day before the phase shift and the indicated day after the phase shift.

Circadian behaviour to assess light-mediated arousal. To assess light-dependent arousal, we entrained the flies for 4 days under 12 h light–12 h dark cycles and then exposed the flies to a 5-min white light pulse (~600 lx LED lights) at ZT22. We binned the activity data for each fly every minute. 'Light-coincident arousal' is the increase in locomotion activity (bin-crosses) during the 5-min stimulation compared to the previous 5 min. 'Arousal delay' is the time between lights on and maximum activity.

Cell transfection, membrane extraction and spectral photometry. The HEK293T cells were obtained from the ATCC, which authenticates their lines. This line has not been tested for mycoplasma contamination. The HEK293T cells were cultured to 70% confluency and transfected with 2 μg pCS2+MT-*rh7* plasmid per 10-cm dish. We used the FuGENE HD Transfection Reagent (Cat.E2311) to perform the transfections. Cells were harvested 24–36 h after transfection and stored at −80 °C. For reconstitution of Rh7 with the chromophore, the HEK293T cells were resuspended in cold PBS (pH 7.4, Quality Biological Inc.) supplemented with a protease inhibitor cocktail (Sigma P8340) and incubated with 40 μM 11-*cis*-retinal in the dark for 4 h. We prepared membrane protein extracts by resuspending membrane pellets in 0.1% CHAPs in PBS, rotating for 2 h at 4 °C, then centrifuging (14,000*g*) for 20 min at 4 °C. The supernatants were removed and analysed with a UV3600 UV-Nir-NIR Spectrometer (Shimadzu). To obtain the spectral absorption for Rh7, we used membrane extracts from untransfected cells as the blank.

ERG recordings. ERG recordings were performed by filling two glass electrodes with *Drosophila* Ringer's solution (3 mM $CaCl_2$, 182 mM KCl, 46 mM NaCl, 10 mM Tris pH 7.2) and placing small droplets of electrode cream on the surface of the compound eye and the thorax to increase conductance. We inserted the recording electrode into the cream on the surface of the compound eye and the reference electrode into the cream on the thorax. Flies were dark adapted for 1 min before stimulating with a 2-s pulse using a halogen light (~30 mV/cm^2 unless indicated otherwise). The ERG signals were amplified with a Warner electrometer and recorded with a Powerlab 4/30 analogue-to-digital converter (AD Instruments). Data were collected and analysed with the Laboratory Chart version 6.1 program (AD Instruments).

Patch-clamp recordings. Patch-clamp measurements were performed on acutely dissected adult fly brains as described previously[18,19]. Briefly, all patch-clamp recordings were performed during the daytime to avoid clock-dependent variance in firing rate. All l-LNvs were recorded within a relatively narrow daytime window, and recordings for each genotype were normally distributed for the time of day and did not vary significantly among all three genotypes. l-LNv recordings were made in whole-cell current clamp mode. After allowing the membrane properties to stabilize after whole cell break-in, we recorded for 30–60 s in the current clamp configuration (unless otherwise stated) under nearly dark conditions (~0.05 mW/cm^2) before the lights were turned on. Lights-on data were collected for 5–20 s and this was followed by 60–120 s of darkness.

Multiple light sources were used for these studies. We used a standard halogen light source on an Olympus BX51 WI microscope (Olympus USA) for all experiments with white light (400–1,000 nm, 4 mW/cm^2). Orange light (550–1,000 nm; 4 mW/cm^2) for electrophysiological recordings was achieved by placing appropriate combinations of 25 mm long- and short-pass filters (Edmund Industrial Optics) over the halogen light source directly beneath the recording chamber. We changed the filters during the recordings to internally match the neuronal responses to different wavelengths of light. Recordings using 405 nm violet light (0.8 mW/cm^2) were obtained using LEDs obtained from Prizmatix 405 LED (UHP-Mic-LED-405), which provide >2 W collimated purple light (405 nm peak, 15 nm spectrum half width). Light was measured for all sources using a Newport 818-UV sensor and the Optical Power/Energy Meter (842-PE, Newport Corporation) and expressed as mW/cm^2.

The control genotype for the electrophysiological recordings was *w;pdf-Gal4-dORK-NC1-GFP*. The cry^{01} and $rh7^1$ recordings were performed using *w;pdf-Gal4-dORK-NC1-GFP;*cry^{01} and *w;pdf-Gal4-dORK-NC1-GFP*; $rh7^1$, respectively.

Statistical analyses. To analyse two sets of data, we used the unpaired Student's *t*-test. To compare multiple sets of behavioural data, we used a one-away ANOVA (Kruskal–Wallis test) followed by Dunn's test. Data are presented as mean ± s.e.m. We used Fisher's exact test to analyse the percentages of rhythmic flies. For the patch-clamp recordings, the data are presented as mean ± s.e.m. Values of *n* refer to the number of measured light on–off cycles. In all cases the *n* values were obtained from at least 5 separate recordings (see legends). ANOVAs were performed using SigmaPlot 11 (Systat Software Inc.) or Prism 6 (Graphpad Software). The data were first tested for normal distribution. If the data were not normally distributed, we performed Kruskal–Wallis one way analysis of variance on ranks, followed by Dunn's test. ANOVAs on normally distributed data were followed by Tukey's test to determine significant differences between genotypes.

Data availability. All data are available from the corresponding author upon reasonable request.

31. Grether, M. E., Abrams, J. M., Agapite, J., White, K. & Steller, H. The *head involution defective* gene of *Drosophila melanogaster* functions in programmed cell death. *Genes Dev.* **9,** 1694–1708 (1995).
32. Emery, P., So, W. V., Kaneko, M., Hall, J. C. & Rosbash, M. CRY, a *Drosophila* clock and light-regulated cryptochrome, is a major contributor to circadian rhythm resetting and photosensitivity. *Cell* **95,** 669–679 (1998).

33. Dolezelova, E., Dolezel, D. & Hall, J. C. Rhythm defects caused by newly engineered null mutations in *Drosophila*'s *cryptochrome* gene. *Genetics* **177,** 329–345 (2007).
34. Yamaguchi, S., Wolf, R., Desplan, C. & Heisenberg, M. Motion vision is independent of color in *Drosophila*. *Proc. Natl Acad. Sci. USA* **105,** 4910–4915 (2008).
35. Vasiliauskas, D. *et al.* Feedback from rhodopsin controls *rhodopsin* exclusion in *Drosophila* photoreceptors. *Nature* **479,** 108–112 (2011).
36. O'Tousa, J. E. *et al.* The Drosophila *ninaE* gene encodes an opsin. *Cell* **40,** 839–850 (1985).
37. Venken, K. J. *et al.* Versatile P[acman] BAC libraries for transgenesis studies in *Drosophila melanogaster*. *Nat. Methods* **6,** 431–434 (2009).
38. Gong, W. J. & Golic, K. G. Ends-out, or replacement, gene targeting in *Drosophila*. *Proc. Natl Acad. Sci. USA* **100,** 2556–2561 (2003).
39. Lee, Y. & Montell, C. *Drosophila* TRPA1 functions in temperature control of circadian rhythm in pacemaker neurons. *J. Neurosci.* **33,** 6716–6725 (2013).
40. Jang, A. R., Moravcevic, K., Saez, L., Young, M. W. & Sehgal, A. *Drosophila* TIM binds importin α1, and acts as an adapter to transport PER to the nucleus. *PLoS Genet.* **11,** e1004974 (2015).
41. Zuker, C. S., Cowman, A. F. & Rubin, G. M. Isolation and structure of a rhodopsin gene from D. melanogaster. *Cell* **40,** 851–858 (1985).
42. Montell, C., Jones, K., Zuker, C. & Rubin, G. A second opsin gene expressed in the ultraviolet-sensitive R7 photoreceptor cells of *Drosophila melanogaster*. *J. Neurosci.* **7,** 1558–1566 (1987).
43. Zuker, C. S., Montell, C., Jones, K., Laverty, T. & Rubin, G. M. A rhodopsin gene expressed in photoreceptor cell R7 of the *Drosophila* eye: homologies with other signal-transducing molecules. *J. Neurosci.* **7,** 1550–1557 (1987).
44. Chou, W. H. *et al.* Identification of a novel Drosophila opsin reveals specific patterning of the R7 and R8 photoreceptor cells. *Neuron* **17,** 1101–1115 (1996).
45. Papatsenko, D., Sheng, G. & Desplan, C. A new rhodopsin in R8 photoreceptors of *Drosophila*: evidence for coordinate expression with Rh3 in R7 cells. *Development* **124,** 1665–1673 (1997).
46. Chou, W. H. *et al.* Patterning of the R7 and R8 photoreceptor cells of *Drosophila*: evidence for induced and default cell-fate specification. *Development* **126,** 607–616 (1999).

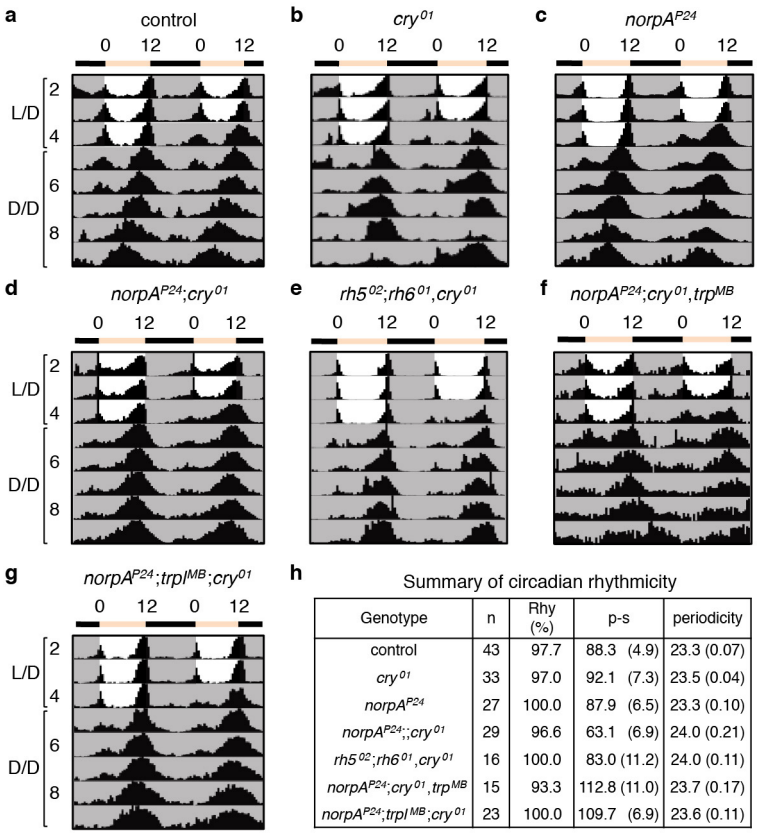

h

Summary of circadian rhythmicity

Genotype	n	Rhy (%)	p-s	periodicity
control	43	97.7	88.3 (4.9)	23.3 (0.07)
cry^{01}	33	97.0	92.1 (7.3)	23.5 (0.04)
$norpA^{P24}$	27	100.0	87.9 (6.5)	23.3 (0.10)
$norpA^{P24};cry^{01}$	29	96.6	63.1 (6.9)	24.0 (0.21)
$rh5^{02};rh6^{01},cry^{01}$	16	100.0	83.0 (11.2)	24.0 (0.11)
$norpA^{P24};cry^{01},trp^{MB}$	15	93.3	112.8 (11.0)	23.7 (0.17)
$norpA^{P24};trpl^{MB};cry^{01}$	23	100.0	109.7 (6.9)	23.6 (0.11)

Extended Data Figure 1 | Circadian photoentrainment in flies lacking cryptochrome and proteins required for phototransduction in the compound eye. a–g, Average actograms exhibited by flies of the indicated genotypes maintained under L–D for 4 days and then released to constant darkness. **h**, Summary of circadian rhythmicity of flies in **a–g**. Rhythm strength of a fly was measured as $p - s$.

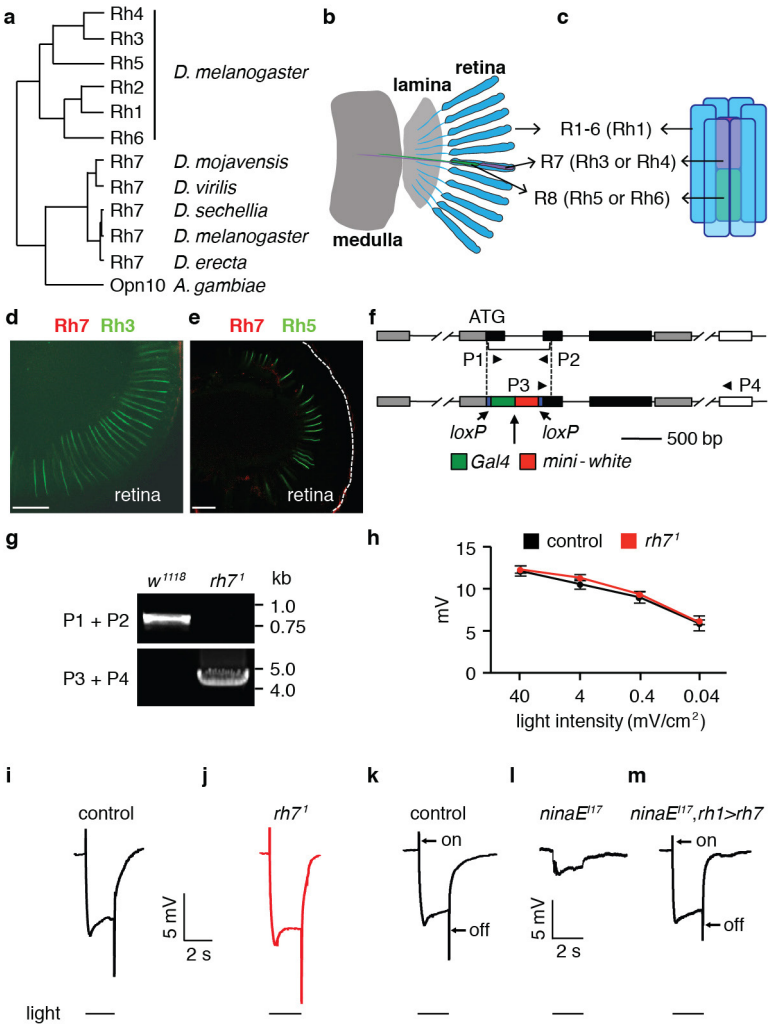

Extended Data Figure 2 | Rh7 is an extraretinal opsin. a, Phylogenetic tree constructed with protein sequences corresponding to the indicated opsins. The full name for *A. gambiae* OP10 is GPROP10 (VectorBase). **b**, Cartoon showing a longitudinal view of the main structures in the *Drosophila* visual system, including the retina, lamina and medulla. The blue units represent ommatidia, which comprise eight photoreceptor cells (R1–8) and support cells. **c**, Cartoon showing the photoreceptor cells in a single ommatidium. The six outer photoreceptor cells (R1–R6) are represented in blue and express Rh1[36,41]. The central R7 photoreceptor cell (purple) expresses Rh3 or Rh4[42,43], while the R8 photoreceptor cell (green) expresses Rh5 or Rh6[44–46]. **d**, A wild-type retina stained with anti-Rh7 (red) and anti-Rh3 (green). **e**, A wild-type retina stained with anti-Rh7 (red) and anti-Rh5 (green). Scale bars, 30 μm. No Rh7-positive staining was detected in the retina. **f**, Generation of $rh7^1$ by homologous recombination. Shown are cartoons of the wild-type *rh7* locus (top) and the genomic organization of the $rh7^1$ allele (bottom). The triangles (P1–P4) indicate the primers used to verify the $rh7^1$ mutation. **g**, Confirmation of the $rh7^1$ mutation by PCR. We prepared genomic DNA from control (w^{1118}) and $rh7^1$ flies and performed PCR using the P1–P2 and P3–P4 primer pairs. The positions of DNA markers (kb) are indicated to the right. See Supplementary Information for the raw images of the PCR gels. **h**, ERG amplitudes of control and $rh7^1$ flies using 2-s white light pulses of the indicated intensities. Error bars indicate s.e.m., $n = 4$. **i–m**, ERGs from flies of the indicated genotypes. The event markers below the ERGs indicate light pulses. **i**, Control flies. **j**, $rh7^1$ flies. **k–m**, Testing for rescue of the reduced ERG amplitude and loss of on- and off-transients in $ninaE^{I17}$ flies with an $rh7^+$ transgene. **k**, Control flies. **l**, $ninaE^{I17}$ (*rh1* mutant). **m**, $ninaE^{I17}$ fly expressing *UAS–rh7* in R1–R6 cells under control of *rh1–Gal4* ($ninaE^{I17}$, *rh1>rh7*).

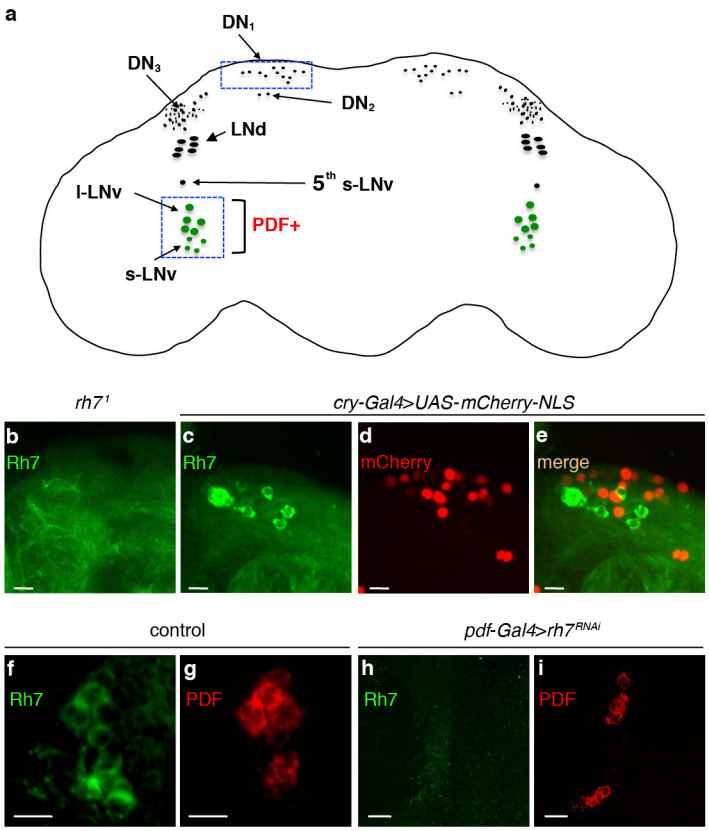

Extended Data Figure 3 | Expression of Rh7 in non-Cry neurons in the dorsal brain. a, Cartoon of a fly brain showing different groups of clock neurons. The boxed areas indicate locations of two groups of Rh7-positive cells. **b**, *rh7*^{1} brain stained with anti-Rh7. **c**–**e**, Double labelling of the dorsal region of the brain with a Cry neuron reporter (*cry–Gal4E13>UAS–mCherry–NLS*) and anti-Rh7. **c**, Anti-Rh7. **d**, Anti-mCherry. **e**, Merge of **c** and **d**. **f**, Control brain stained with anti-Rh7. **g**, Control brain stained with anti-PDF. **h**, *pdf-Gal4>rh7*^{RNAi} brain stained with anti-Rh7. **i**, *pdf-Gal4>rh7*^{RNAi} brain stained with anti-PDF. Scale bars: **b**–**e**, 20 μm; **f**–**i**, 10 μm.

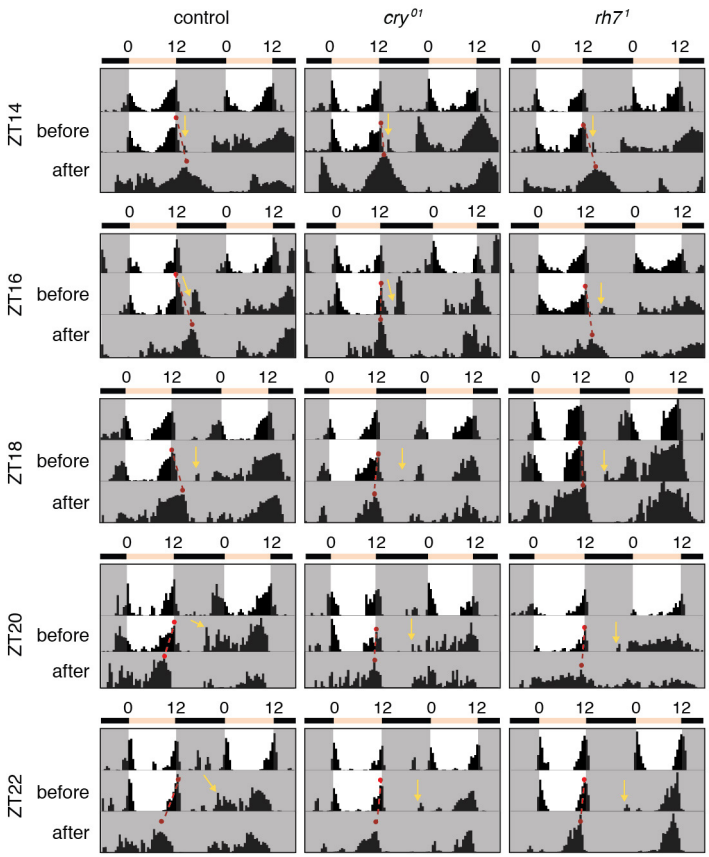

Extended Data Figure 4 | Actograms showing representative behaviour of control and mutant flies before and after a 5-min light pulse at the indicated ZT. Red dots connected by dashed red lines indicate evening peaks before and after the light pulse. Each yellow arrow indicates exposure to a 5-min ~600 lx LED light pulse.

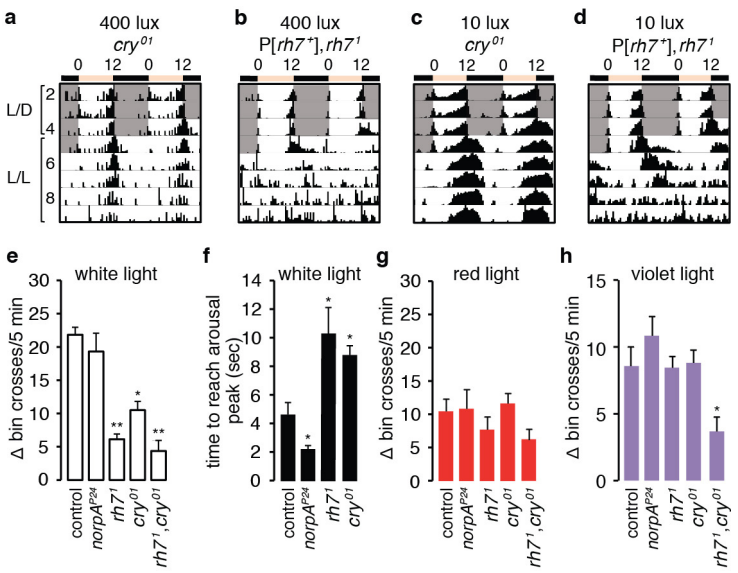

Extended Data Figure 5 | Circadian responses to constant light and light-dependent arousal in *rh7*^{1} flies. a, **b**, Flies of the indicated genotypes were entrained under L–D cycles and subsequently released to constant ~400 lx light (L–L). **c**, **d**, Flies of the indicated genotypes were entrained under L–D cycles and subsequently released to constant ~10 lx light (L–L). **e**, Quantification of the effect of a 5-min white light pulse on arousal. Arousal was quantified as increases in total bin crosses during the 5-min light stimulation compared to the total bin crosses during the 5 min before light stimulation. **f**, Quantification of the time required to reach maximum activity after white light stimulation. **g**, **h**, Quantification of the effects on arousal of a 5-min exposure to red (625 nm) (**g**) or violet (405 nm) LED lights (**h**). Error bars indicate s.e.m. One-away ANOVA (Kruskal–Wallis test) followed by Dunn's test. $*P < 0.05$, $**P < 0.01$. Number of flies tested: *norpA*^{P24}, $n = 16$; other genotypes, $n = 24$.

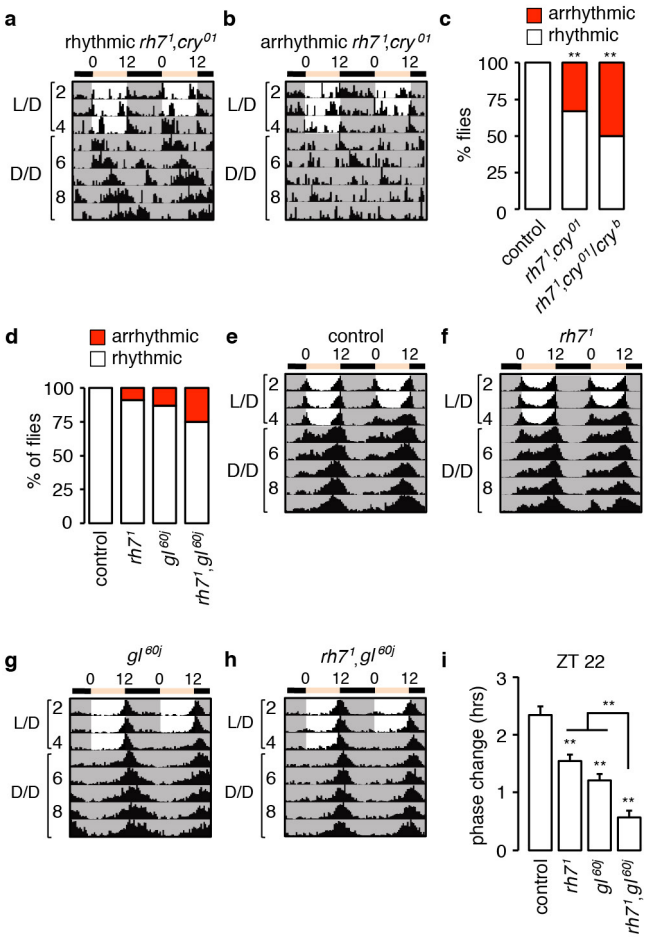

Extended Data Figure 6 | Effects of multiple light input pathways on circadian behaviour. a, **b**, Actograms showing rhythmic and arrhythmic *rh7*^{1} *cry*^{01} double mutants. The flies were entrained under L–D cycles and subsequently released to constant darkness. **c**, Percentages of rhythmic and arrhythmic flies. Fisher's exact test, $^{**}P < 0.01$. Number of flies tested: control, $n = 16$; other genotypes, $n = 30$. **d**–**h**, Circadian behaviour of *gl*^{60j} and *rh7*^{1} *gl*^{60j} double mutant flies. The flies were entrained to L–D cycles for 4 days and subsequently released to constant darkness. **d**, Percentages of rhythmic and arrhythmic flies. **e**–**h**, Average actograms showing the activities of flies of the indicated genotypes. Number of flies tested: control, $n = 46$; *rh7*^{1}, $n = 34$; *gl*^{60j}, $n = 38$; *rh7*^{1} *gl*^{60j}, $n = 40$. **i**, Phase response of the indicated genotypes to 5-min white light stimulation at ZT22. Error bars indicate s.e.m. One-way ANOVA (Kruskal–Wallis test) followed by Dunn's test. $^{**}P < 0.01$. Flies tested: control, $n = 54$; *rh7*^{1}, $n = 49$; *gl*^{60j}, $n = 53$; *rh7*^{1} *gl*^{60j}, $n = 57$.

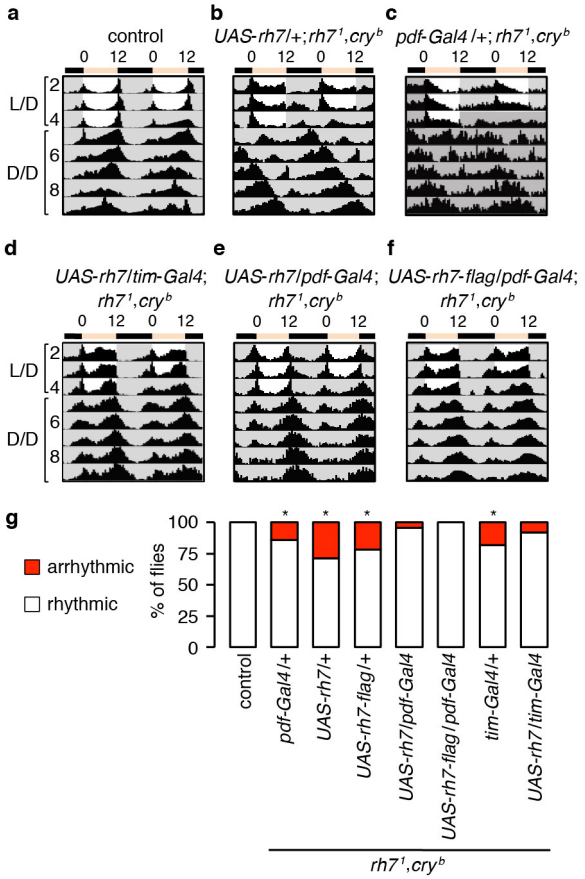

Extended Data Figure 7 | Rescue of the *rh7¹ cryᵇ* photoentrainment defect by expression of *rh7* in pacemaker neurons. a–c, Actograms of control flies and *rh7¹ cryᵇ* flies harbouring only the *UAS–rh7* or *pdf–Gal4* transgenes. Number of flies tested: control, $n = 16$; *UAS–rh7/+*; *rh7¹ cryᵇ*, $n = 52$; *pdf–Gal4/+*; *rh7¹ cryᵇ*, $n = 21$. **d–f**, Actograms of *rh7¹ cryᵇ* flies expressing *UAS–rh7* in pacemaker neurons under the control of *tim–Gal4* or *pdf–Gal4* as indicated. Number of flies tested: *UAS–rh7/tim–Gal4;rh7¹ cryᵇ*, $n = 37$; *UAS–rh7/pdf–Gal4; rh7¹ cryᵇ*, $n = 23$; *UAS–rh7–flag/pdf–Gal4;rh7¹ cryᵇ*, $n = 21$. **g**, Percentages of rhythmic and arrhythmic flies of the indicated genotypes. Fisher's exact test, $^*P < 0.05$.

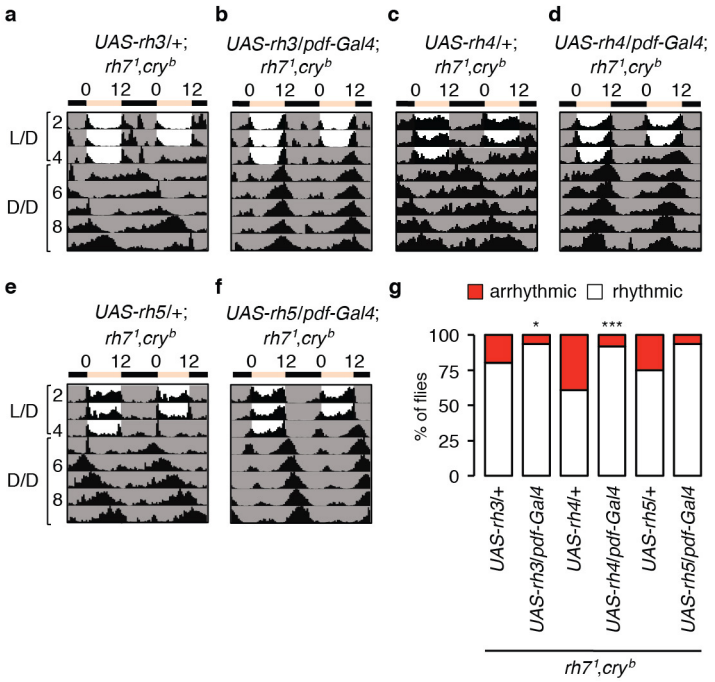

Extended Data Figure 8 | Rescue of *rh7¹ cryᵇ* photoentrainment defect by expression of other fly rhodopsins. a–f, Controls showing actograms of *rh7¹ cryᵇ* flies harbouring *UAS–rhodopsin* transgenes only, and of *rh7¹ cryᵇ* flies expressing the indicated rhodopsin genes in pacemaker neurons under the control of *pdf–Gal4*. Number of flies tested: *UAS–rh3/+;rh7¹ cryᵇ*, $n = 56$; *UAS–rh4/+;rh7¹ cryᵇ*, $n = 46$; *UAS–rh5/+;rh7¹ cryᵇ*, $n = 24$; *UAS–rh3/pdf–Gal4;rh7¹ cryᵇ*, $n = 64$; *UAS–rh4/pdf–Gal4;rh7¹ cryᵇ*, $n = 25$; *UAS–rh5/pdf–Gal4;rh7¹ cryᵇ*, $n = 16$. **g**, Percentages of rhythmic and arrhythmic flies of the indicated genotypes. Fisher's exact test, $^{*}P < 0.05$, $^{***}P < 0.001$.

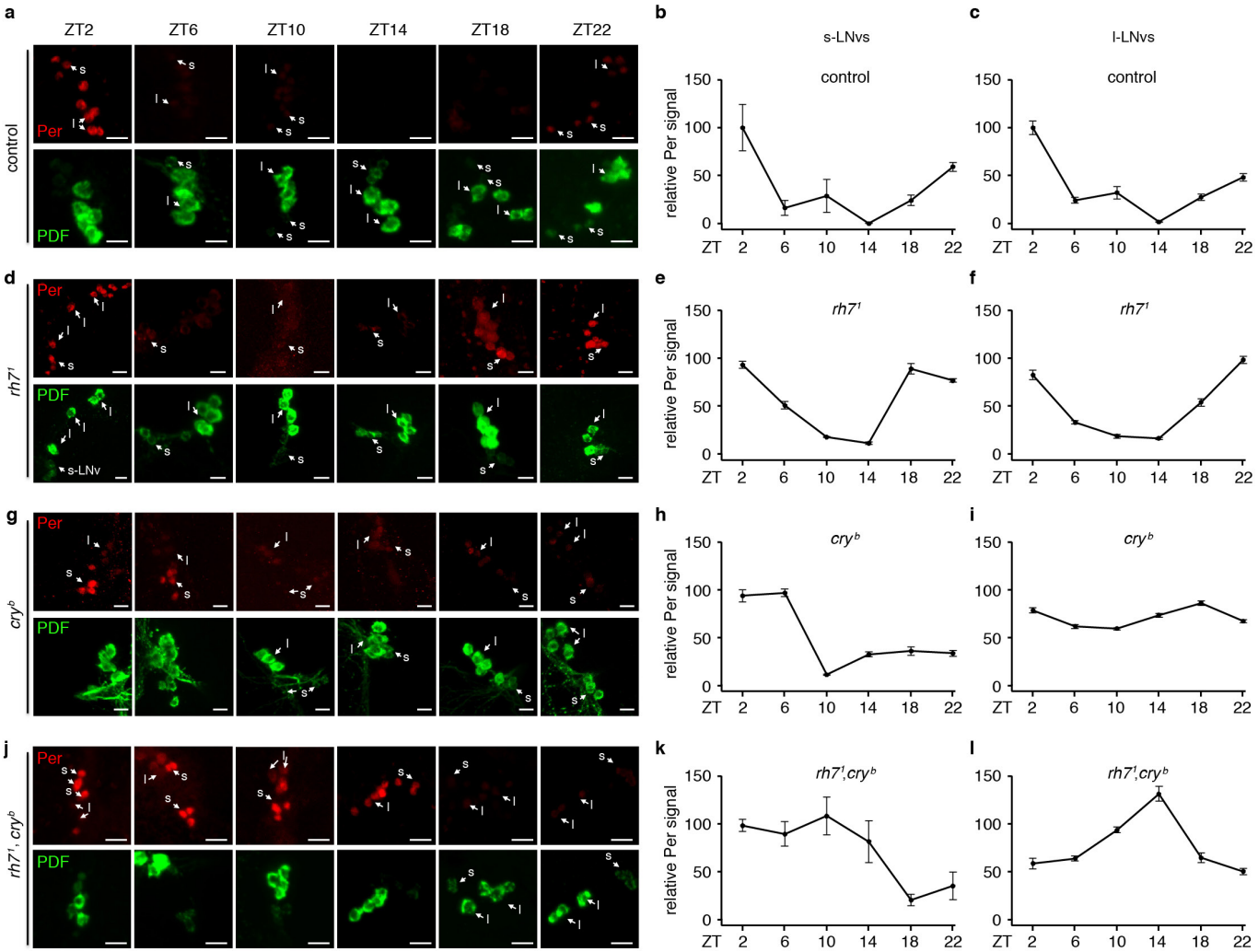

Extended Data Figure 9 | Per oscillates in control, *rh7¹*, *cry^b* and *rh7¹ cry^b* flies. a, **d**, **g**, **j**, Flies of the indicated genotypes were entrained under L–D cycles for 4 days and the brains were dissected on the 5th day. The ZT times indicate when the brains were fixed and dissected for staining with anti-Per (Per, upper rows, red) and anti-PDF (PDF, lower rows, green) as indicated. At least one s-LNV (s) and one l-LNV (l) are labelled in the images obtained at each ZT to facilitate identification of LNVs. Scale bars, 10 μm. **b**, **c**, **e**, **f**, **h**, **i**, **k**, **l**, Quantification of relative Per levels in s-LNvs and L-LNVs of flies of the indicated genotypes. The image quantification was performed using ImageJ. The *y* axes indicate relative Per intensities. The Per intensities in ZT2 of the control flies were designated as 100. For control flies, ZT10, $n = 6$; ZT22, $n = 8$; $n = 5$ for all other time points. For *rh7¹*, ZT2, $n = 9$; ZT6, $n = 8$; ZT10, $n = 6$; ZT14, $n = 8$; ZT18, $n = 8$; ZT22, $n = 7$. For *cry^b*, ZT2, $n = 8$; ZT6, $n = 9$; ZT10, $n = 8$; ZT14, $n = 7$; ZT18, $n = 10$; ZT22, $n = 8$. For *rh7¹ cry^b*, $n = 5$ for all time points. Error bars indicate s.e.m.

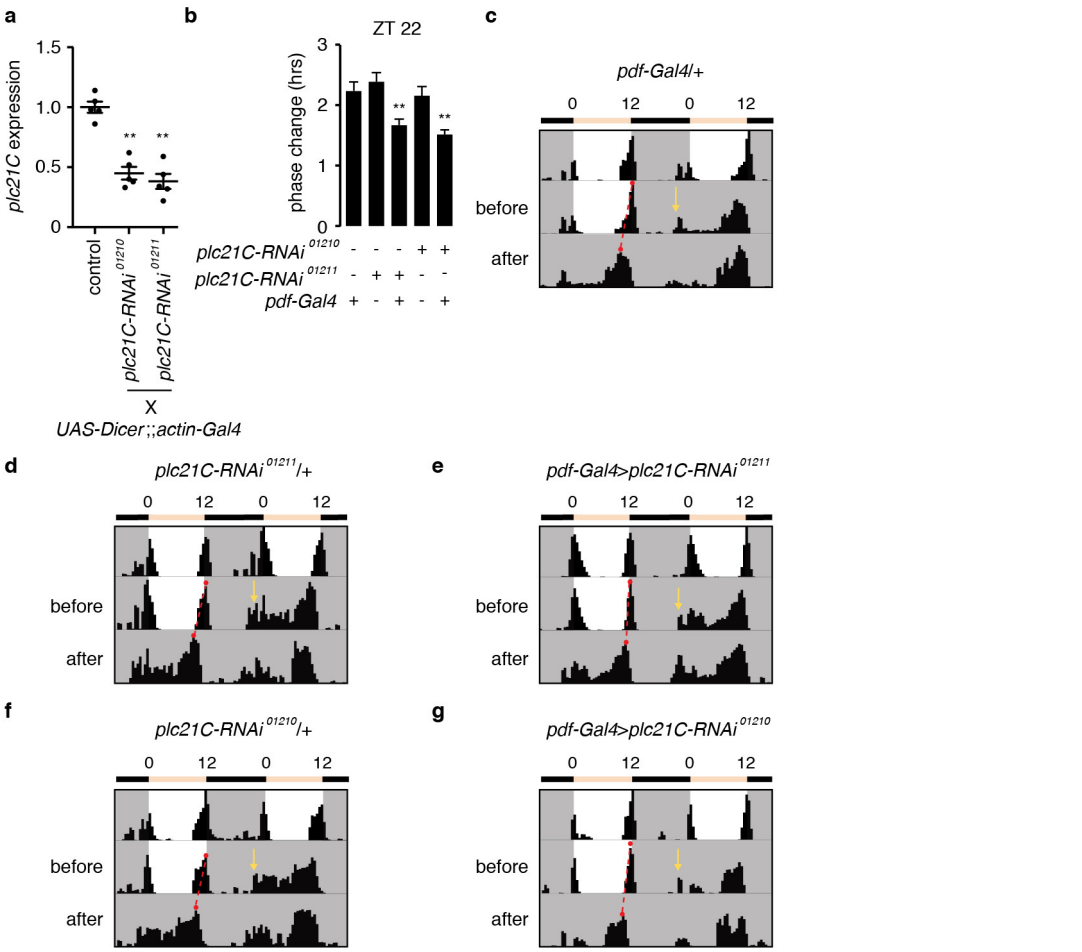

Extended Data Figure 10 | Knockdown of *plc21C* in PDF-positive neurons impaired circadian phase response. a, Quantitative real-time PCR analysis of *plc21C* mRNA using RNA prepared from whole adults. The *plc21C* expression levels in each sample were normalized using *rp49* expression. The control was w^{1118}. Centre values indicate the average and error bars indicate s.e.m. One-away ANOVA (Kruskal–Wallis test) followed by Dunn's test. $^{**}P < 0.01$. **b**, Phase response of the indicated genotypes to 5 min white light stimulation at ZT22. One-away ANOVA (Kruskal–Wallis test) followed by Dunn's test. $^{**}P < 0.01$. *pdf–Gal4/+*, $n = 32$; *plc21C–RNAi*^{01211}*/+*, $n = 31$; *pdf–Gal4>plc21C–RNAi*^{01211}, $n = 37$; *plc21C–RNAi*^{01210}*/+*, $n = 15$; *pdf–Gal4>plc21C–RNAi*^{01210}, $n = 32$. Error bars indicate s.e.m. **c**–**g**, Examples of behaviour before and after the 5-min light pulse. The yellow arrows indicate the times of the 5-min white light pulses (~600 lx). The red dots connected by dashed red lines indicate the evening peaks before and after the light pulse.